Accurate RR-Interval Detection with Daubechies Filtering and Adaptive Thresholding

Mochammad Rif'an, Robert Rieger and Chua-Chin Wang

Abstract QRS detection is needed for electrocardiogram (ECG) signal analysis, including the Heart Rate Variability (HRV) analysis, which is the physiological phenomenon of variation of the time intervals between two consecutive heartbeats. R is the point corresponding to the peak of a QRS complex of ECG waves. RR-interval is defined as the interval between two successive Rs. We proposed an algorithm to acquire RR-interval based on a level-4 Stationary Wavelet Transform (SWT) to decompose ECG signal followed by an adaptive thresholding algorithm to separate QRS complex from other unwanted signals. Daubechies filter is chosen as the mother wavelet, because its shape of the scaling function resembles a QRS complex. The proposed algorithm is simulated by MATLAB, where 48 files from MIT-BIH arrhythmia database are used as benchmarks to verify the algorithm. Simulation results show 99.64% of sensitivity and 99.48% of positive predictivities.

Keywords QRS peaks · RR-interval · Stationary wavelet transform · Daubechies · Adaptive thresholding

1 Introduction

Recently, many people have paid attention to their health, particularly the heart condition. The arrhythmia is one of the heart-related diseases needed to be monitored periodically. It is a problem with the irregular rate of the heart beats. It might be too quick, too slow, or non-periodical. To analyze whether the heart rate is normal or not, it needs to extract features from ECG signals, and the accurate detection of the QRS complex is the critical task in ECG wave analysis, including HRV analysis. HRV is the physiological phenomenon of variation of the time

M. Rif'an · C.-C. Wang (✉)
National Sun Yat-Sen University, Kaohsiung 80424, Taiwan
e-mail: ccwang@ee.nsysu.edu.tw

R. Rieger
Kiel University, Kiel, Germany

interval between two consecutive heartbeats. Notably, R is the peak of a QRS complex such that RR-interval is defined as the interval between successive Rs. It can indicate many health-related syndromes such as arrhythmia. Many researchers have developed techniques regarding QRS peak detection or RR-interval acquisition. Bayasi, et al. isolated QRS energy centered at 10 Hz with band-pass filtering the raw ECG signal [1]. The filter is composed of low-pass and high-pass filters. Differentiation is then used to find out the high slope such that the QRS complex can be extracted. Zhang, et al. proposed a Pulse-Triggered (PUT) and time-assisted PUT (t-PUT) approach based on the level-crossing events [2]. An event driven by "fall" and "rise" notes is used to detect the QRS complex. Tang, et al. proposed a parallel delta modulator architecture with local maximum point and minimum point detection algorithms to detect QRS and PT waves [3]. A delta modulator represents the slope of the input with a three-state bit stream. Rising, falling, and the difference between rising and falling labels are used as the bit stream.

To resolve the mentioned problems, an RR-interval acquisition using Stationary Wavelet Transform (SWT) followed by an adaptive thresholding algorithm and a peak detector with slope identification is proposed in this study. Thorough simulation with arrhythmia ECG benchmarks is demonstrated to justify the proposed method

2 Accurate RR-Interval Estimation Approach Based on Swt and Adaptive Threshold

Figure 1 shows the flowchart of the proposed method. The discrete ECG signal is decomposed by the SWT to remove noise outside of the desired band. An adaptive thresholding is then applied to separate the QRS wave pattern from the rest. R is the peak of a QRS wave, which needs a peak detector to find out the R-peak point. The proposed method is implemented using MATLAB software and then downloaded to FPGA for hardware verification

Fig. 1 Flow chart of the proposed algorithm for RR-interval estimation
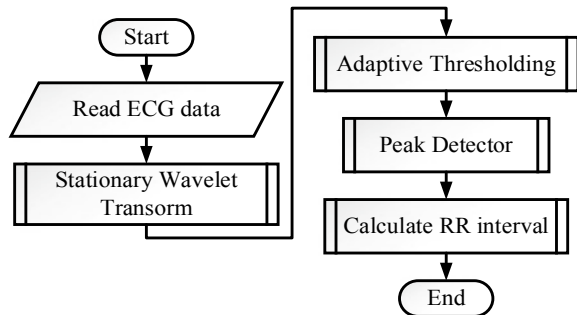
2.1 Wavelet Transform

Theoretically, the signal in time domain or frequency domain can be analyzed by wavelet transforms, particularly, a finite length or fast decaying oscillation signals. The wavelet transform of a signal $f(t)$ is governed by the following Eq. (1):

$$Wf(a, b) = \frac{1}{\sqrt{a}} \int\limits_{-\infty}^{+\infty} f(t) \psi \left(\frac{t - b}{a} \right) dt \tag{1}$$

where $((t - b)/a)$ is the mother/base wavelet with dilation 'a' and translation 'b'. The higher a, the wider wavelet basis function such that this wavelet coefficient provides low frequency information [4]. For discrete-time signals, the dyadic Discrete Wavelet Transform (DWT) is equivalent, according to Mallat's algorithm, to an octave filter bank [5], which can be implemented as a cascaded of identical cells, e.g., low-pass and high-pass Finite Impulse Response (FIR) filters.

2.2 Stationary Wavelet Transform (SWT)

The typical Discrete Wavelet Transform (DWT) decimates the wavelet coefficients at each level. Thus, the results of the wavelet transform at each level are half the size of the original sequence. The Stationary Wavelet Transform (SWT), on the other hand, pads the corresponding low-pass and high-pass filters with zeros and two new sequences resulting in the generation of the same length as the original sequence [6]. SWT has no decimation in the time domain. By contrast, only a dyadic subsampling of scales (frequency domain) is performed. Hence, it is featured with translation invariance and without resolution loss at lower frequencies, which are major bottlenecks for DWT [6, 7]. Although it increases redundancy in coefficients, the additional artifacts caused by time-domain subsampling at higher scales are avoided.

Based upon the above analysis, SWT with the Daubechies [8, 9] as base/mother wavelet is adopted in this work, because the shapes of the scaling function are close to that of the QRS complex. Low Pass Filter (LPF) for the Daubechies is shown as follows [9]:

$$H_\varphi \left(e^{j\omega} \right) = \sqrt{2} \left(\frac{1 + e^{-j\omega}}{2} \right)^p R \left(e^{j\omega} \right) \tag{2}$$

where p is vanishing moments [9], and $R(e^{j\omega})$ is a polynomial. The mother wavelet with vanishing moment 3 is chosen because it has a moderate short filter that the computational complexity is low. Notably, the QRS complex power density is positioned in the range of 2–20 Hz, where the maximum is at about 12 Hz [10, 11]. The maximum power spectra of QRS complex is around 8–12 Hz.

Fig. 2 Frequency response of details from db3 SWT
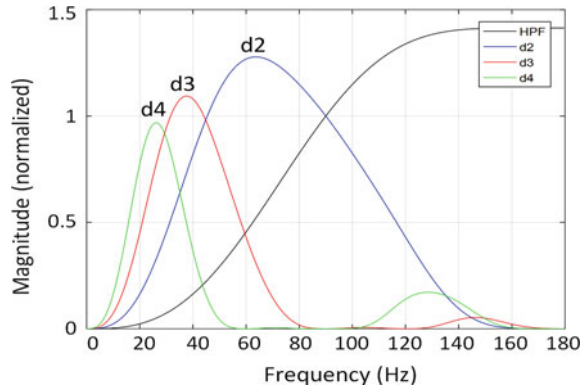
Figure 2 shows the frequency response for several Stationary wavelet transform coefficients with Daubechies as mother wavelet for 360 Hz sampling frequency. The closest bandwidth to the frequency of QRS signals is the level 4 (d4) of SWT with 3 dB bandwidth around 18–34 Hz with the moderate length of filters. Apparently, it is the best choice to enhance the QRS complexes and suppress other unwanted signals or noises, since the R-peak is the only subject for the detection of the interval.

2.3 Adaptive Thresholding

The straight forward thought to detect the R-peaks position at level-4 (d4) is to use a threshold. However, the value of the R-peaks at d4 varies along with the time. An adaptive thresholding method is proposed to resolve the time variant issue, where a moving average is calculated as the threshold for the detection of peaks. Figure 3 shows an example of the thresholding, where an average window is sliding along time axis. All d4 coefficients are averaged inside the window. The adaptive threshold value is then generated as the red line, namely the moving average of d4.
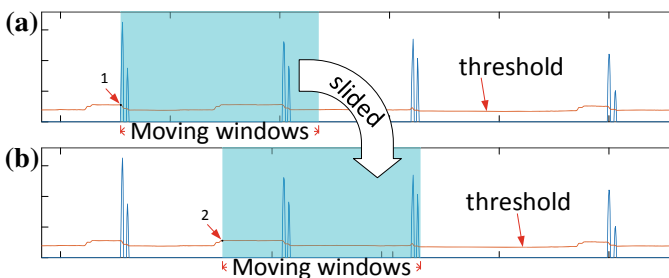
Fig. 3 Moving windows for threshold calculation, **a** at point 1; **b** at point 2

All d4 values below the threshold are reset to zero. By contrast, the data with values over or equal to the threshold are kept the same. Therefore, the d4 processed by the thresholding becomes the blue line in Fig. 3. Notably, the adaptive thresholding is fixed when initialized. This will cause false result for the first beat, because there is no value for d4 at this stage along the look back window.

2.4 Peak Detector

Referring to Fig. 1, the next step of the proposed method is peak detection. Figure 4 shows the peak detector algorithm, where the current data is compared with the previous data such that the slope of these two data is calculated. If the slope is positive, it indicates that the trend is rising, not the peak. By contrast, if the current slope is negative, but the previous slope is positive, the peak is found. The last case is that the current slope and the previous one are both negative.

3 Experiments

A total of 48 records from MIT-BIH arrhythmia database (mtdb) [12] of Physiobank ATM are used for verification. The ECG signals are digitized as 360 samples per second in one channel, where the resolution and voltage range are 11 bits and 10 mV, respectively. All the recordings are annotated independently by cardiologists, which provide reliable and accurate annotation information of each heart beat. Table 1 tabulates the simulation results by the proposed algorithm.

Fig. 4 Peak detector flowchart
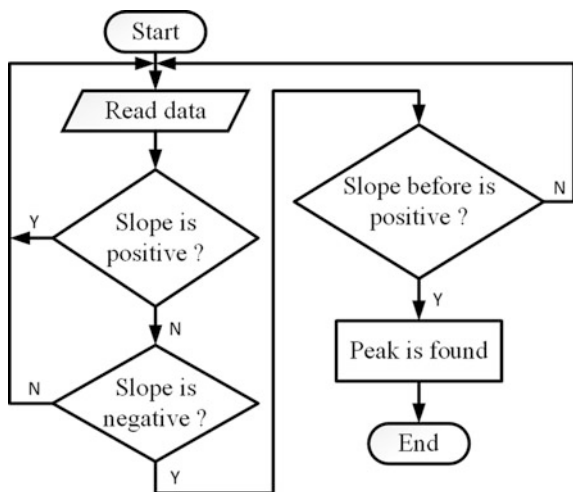
Table 1 Summary of performance indexes for 48 records

No	Rec.	FP	FN	TP	Se (%)	P+ (%)	Error (%)
1	100	0	0	2272	100.00	100.00	0.00
2	101	5	0	1864	100.00	99.73	0.27
3	102	0	0	2186	100.00	100.00	0.00
4	103	0	0	2083	100.00	100.00	0.00
5	104	26	0	2228	100.00	98.85	1.17
6	105	22	1	2570	99.96	99.15	0.89
7	106	6	18	2008	99.11	99.70	1.18
8	107	0	0	2136	100.00	100.00	0.00
9	108	36	3	1759	99.83	97.99	2.21
10	109	0	4	2527	99.84	100.00	0.16
11	111	2	1	2122	99.95	99.91	0.14
12	112	1	0	2538	100.00	99.96	0.04
13	113	17	0	1794	100.00	99.06	0.95
14	114	8	0	1878	100.00	99.58	0.43
15	115	0	0	1952	100.00	100.00	0.00
16	116	26	30	2381	98.76	98.92	2.32
17	117	0	0	1534	100.00	100.00	0.00
18	118	1	0	2277	100.00	99.96	0.04
19	119	0	0	1986	100.00	100.00	0.00
20	121	0	1	1861	99.95	100.00	0.05
21	122	0	0	2475	100.00	100.00	0.00
22	123	1	0	1517	100.00	99.93	0.07
23	124	1	0	1618	100.00	99.94	0.06
24	200	9	2	2598	99.92	99.65	0.42
25	201	41	4	1958	99.80	97.95	2.29
26	202	1	3	2132	99.86	99.95	0.19
27	203	13	42	2937	98.59	99.56	1.85
28	205	0	4	2651	99.85	100.00	0.15
29	207	13	246	2085	89.45	99.38	11.11
30	208	6	22	2932	99.26	99.80	0.95
31	209	0	0	3004	100.00	100.00	0.00
32	210	4	15	2634	99.43	99.85	0.72
33	212	0	0	2747	100.00	100.00	0.00
34	213	0	1	3249	99.97	100.00	0.03
35	214	2	1	2260	99.96	99.91	0.13
36	215	0	2	3360	99.94	100.00	0.06
37	217	6	5	2202	99.77	99.73	0.50
38	219	1	0	2153	100.00	99.95	0.05
39	220	0	0	2047	100.00	100.00	0.00
40	221	0	3	2423	99.88	100.00	0.12

Table 1 (continued)

No	Rec.	FP	FN	TP	Se (%)	P+ (%)	Error (%)
41	222	4	0	2482	100.00	99.84	0.16
42	223	1	0	2604	100.00	99.96	0.04
43	228	44	4	2048	99.81	97.90	2.34
44	230	2	0	2255	100.00	99.91	0.09
45	231	1	0	1570	100.00	99.94	0.06
46	*232*	*215*	*0*	*1779*	*100.00*	*89.22*	*12.09*
47	233	0	5	3073	99.84	100.00	0.16
48	234	0	0	2752	100.00	100.00	0.00
		515	417	109,501	99.64	99.48	0.89

Three indexes, the sensitivity (*Se*), Positive Predictivity (*P+*), and Error are used to compare the performance as follows:

$$Se = \frac{TP}{TP + FN} \tag{3}$$

$$P^+ = \frac{TP}{TP + FP} \tag{4}$$

$$Error = \frac{FP + FN}{TP + FN + FP} \times 100 \tag{5}$$

The worst result is the false negative of record file 207, as shown in Fig. 5. The output of d4 by SWT can distinguish the QRS complex, though the R peaks are in reverse positions (Fig. 5a) relative to the yellow line Fig. 5b. However, when the noise (pointer 1) and R peaks position (pointer 2) are close, it needs an optimum value for the moving average to tell the difference. The peak detector demonstrates a good result in Fig. 5c to resolve this difficulty.
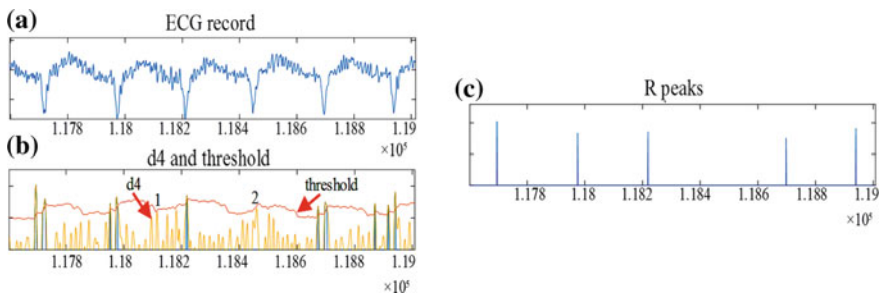
Fig. 5 A part of ECG record file number 207 from MIT-BIH; **a** the original signal; **b** d4 before adaptive thresholding (yellow), after thresholding (blue), and the threshold (red); **c** detected R-peak positions

Notably, the false positive of record file 232 is another issue, where the R-peak values are smaller than the threshold. The noise makes the moving average increase significantly. The key to find the optimum result is the adaptive thresholding, especially the optimum width of the moving window. The average of Se and p+ shown in Table 1 have similar results. It is concluded that the chosen value is near to the optimum one.

To justify the feasibility, the proposed algorithm is implemented and downloaded onto an FPGA (Artic-7). A QRS complex part of record file 100 MIT-BIH arrhythmia as input data (top) is shown in Fig. 6, where clock (clk) period is 100 ns. Peak detection is shown in the bottom strip. There is a delay between two consecutive peaks (R-peaks), which is around several clocks. It is caused by the hardware delay in wavelet implementation. Meanwhile, these peaks at the beginning are not accountable, because the moving average thereof for the dynamic threshold is not reliable.

Performance evaluation of the QRS detector is compared with 3 prior works as shown in Table 2. The values not listed in the reference are written with "n.a.".
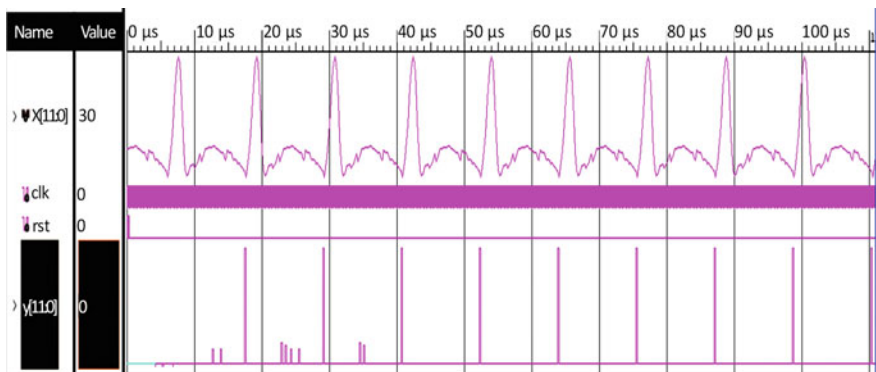
Fig. 6 A part of ECG record file number 100 from MIT-BIH (above), and R-peak position (below)

Table 2 Performance comparison with other method

QRS detector	Technique	TP	FN	FP	Error (%)	Se (%)	P+ (%)
TBCAS [2], 2014	Pulse-triggered	109,966	2665	3015	n.a.	97.63	97.76
ICEE [13], 2017	Level-crossing sampling	n.a.	n.a.	n.a.	1.71	98.89	99.4
TBCAS [3], 2018	Parallel delta modulator	109,966	911	494	1.28	99.17	99.55
This work, 2018	SWT, dynamic threshold	109,501	515	417	0.89	99.64	99.48

Although all of the listed methods have similarity Se and P+, our work demonstrates 0.89% error, which is the best of all.

4   Conclusions

An RR-interval acquisition approach has been presented in this investigation. The algorithm is composed of SWT, moving average for adaptive thresholding, and filtering. 48 records from MIT-BIH arrhythmia database are tested to verify the correctness of the algorithm. 99.64 and 99.48% of sensitivity and positive predictivity for RR-interval estimation are justified, respectively. Last but not least, the proposed algorithm is also successfully implemented by FPGA to prove the feasibility, and the best of 0.89% error

References

1. Bayasi N, Saleh N, Mohammad B, Ismail M (2014) 65-nm ASIC implementation of QRS detector based on Pan and Tompkins algorithm. In: 10th International conference on innovations in information technology (IIT). Al Ain, United Arab Emirates, 9–11 Nov 2014, pp 84–87
2. Zhang X, Lian Y (2014) A 300-mV 220-nW event-driven ADC with real-time QRS detection for wearable ECG sensors. IEEE Trans Biomed Circ Syst 8(6):834–843
3. Tang X, Hu Q, Tang W (2018) A real-time QRS detection system with PR/RT interval and ST segment measurements for wearable ECG sensors using parallel delta modulators. IEEE Trans Biomed Circ Syst 12(4):751–761
4. Mallat S (2009) A wavelet tour of signal processing. Academic, New York
5. Mallat S (1989) Multifrequency channel decompositions of images and wavelet models. IEEE Trans Acoust Speech Sig Process 37(12):2091–2110
6. Nason G, Silverman B (1995) The stationary wavelet transform and some statistical applications. University of Bristol
7. Merah M, Abdelmalik TA, Larbi BH (2016) R-peaks detection based on stationary wavelet transform. Comput Methods Programs Biomed 121(3):149–160
8. Daubechies I (1988) Orthonormal bases of compactly supported wavelets, communications on pure and applied mathematics, vol XLI, pp 909–996
9. Liu C-L (2010): A tutorial of the wavelet transform
10. Thakor NV, Webster JG, Tompkins W (1983) Optimal QRS detector. Med Biol Eng Comput 21(3):343–350
11. Webster JG (2010) Medical instrumentation application and design. Wiley, New York
12. Physionet. PhysioBank ATM homepage. https://www.physionet.org/cgi-bin/atm/ATM. Last accessed on 23 Sept 2018
13. Ravanshad N, Rezaee-Dehsorkh H (2017) An event-based ECG-monitoring and QRS-detection system based on level-crossing sampling. In: 2017 Iranian conference on electrical engineering (ICEE), Tehran, pp 302–307